Shear Design of Prestressed Concrete: A Unified Approach

Tyler S. Wolf[1] and Robert J. Frosch, Ph.D, P.E., M.ASCE[2]

Abstract: Design methods for the shear resistance of reinforced and prestressed concrete beams are based on empirical evidence. Due to different approaches in their development, different equations are used to calculate the shear strength of reinforced and prestressed concrete. Recent research has provided a simplified approach for the shear design of reinforced concrete that eliminates many of the shortcomings of current design procedures and corresponds well to a wide range of test results. The objective of this research was to investigate the applicability of this new approach to prestressed concrete. The applicability of the shear model was evaluated by a comparison of its results with the experimental strengths of 86 specimens which failed in shear. This investigation indicated that the shear model is applicable to prestressed sections. For design purposes, the shear model was simplified to develop a design expression that unifies the design of reinforced and prestressed concrete sections.

DOI: 10.1061/(ASCE)0733-9445(2007)133:11(1512)

CE Database subject headings: Concrete, reinforced; Shear strength; Concrete, prestressed.

Introduction

The behavior of structural concrete beams subjected to shear has been investigated since the advent of reinforced concrete. Due to the number of variables involved, however, a general shear theory has been evasive. Consequently, design is based on empirical evidence which has resulted in a multitude of design equations for the design of structures in shear. For instance, the ACI 318 Building Code (ACI 318 2005) provides five different equations to evaluate the concrete contribution to shear resistance, V_c, for nonprestressed members and three different equations to evaluate V_c for prestressed members. To calculate V_c according to the AASHTO design specifications is dependent on the version of specifications used. In general, the 17th Ed. of the *Standard Specifications* (AASHTO 2002) conforms to the ACI building code. However, the AASHTO LRFD (AASHTO 2005) bridge design specifications introduced substantially different provisions for shear design and provided a new method that designers must consider.

The AASHTO LRFD specifications are based on the modified compression field theory and on strut-and-tie modeling. There are advantages to the LRFD method such as unified treatment of nonprestressed and prestressed members. However, the LRFD specifications have been identified as being complex, requiring time-consuming iteration, producing illogical answers in some situations, and providing excessive amounts of reinforcement for certain cross sections (NCHRP 2002). ACI 318, while generally providing ease in calculation, has also been identified as having several shortcomings including lack of conservatism for lightly reinforced cross sections, for sections utilizing high strength concrete, and for large sections (Reineck et al. 2003; Tompos and Frosch 2002).

Recent research has developed a model and simplified design equation for calculating the shear strength of nonprestressed members which eliminates many of the shortcomings of current design methods (Tureyen and Frosch 2003). The equation recommended for the design of nonprestressed members is as follows

$$V_c = 5\sqrt{f'_c}b_w c \quad (V_c = 0.42\sqrt{f'_c}b_w c) \tag{1}$$

The applicability of this design equation is supported by comparing the computed shear strengths with the experimental strengths of 339 specimens as shown in Fig. 1. As an additional benefit, the design equation was shown to be applicable to both steel and fiber reinforced polymer (FRP) bar reinforced beams. The effective reinforcement ratio is plotted on the horizontal axis which is simply the reinforcement ratio (ρ) multiplied by the modular ratio to account for the varying modulus of elasticity of FRP reinforcement. This design equation is simple and shown to provide conservative results while maintaining a fairly uniform factor of safety.

To provide perspective on the improvement provided by this equation, Fig. 2 presents results provided by the commonly used design equation

$$V_c = 2\sqrt{f'_c}b_w d \quad (V_c = 0.17\sqrt{f'_c}b_w d) \tag{2}$$

As shown, the factor of safety varies with the effective reinforcement ratio, and unconservative results can be obtained for low ratios, especially FRP reinforced beams which have low ratios resulting from the modulus of elasticity of this reinforcement type.

Research Objective

The objective of this study was to investigate the applicability of the shear model and simplified design method developed for re-

[1]Bridge Engineer, Beam, Longest, and Neff, 8126 Castleton Rd., Indianapolis, IN 46250. E-mail: twolf@b-l-n.com

[2]Associate Professor, Dept. of Civil Engineering, Purdue Univ., 550 Stadium Mall Dr., West Lafayette, IN 47907 (corresponding author). E-mail: frosch@purdue.edu

Note. Associate Editor: Yahya C. Kurama. Discussion open until April 1, 2008. Separate discussions must be submitted for individual papers. To extend the closing date by one month, a written request must be filed with the ASCE Managing Editor. The manuscript for this paper was submitted for review and possible publication on February 14, 2006; approved on June 2, 2006. This paper is part of the ***Journal of Structural Engineering***, Vol. 133, No. 11, November 1, 2007. ©ASCE, ISSN 0733-9445/2007/11-1512–1519/$25.00.

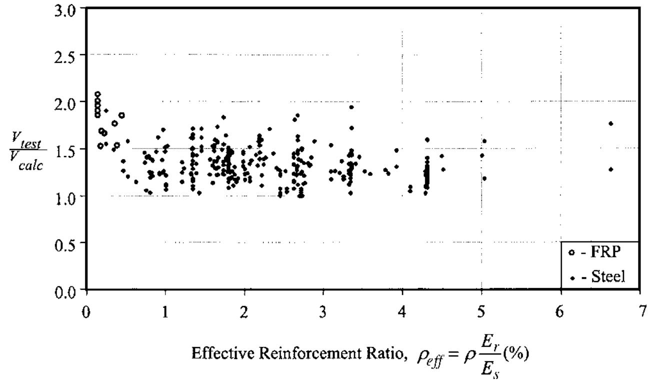

Fig. 1. Results of Eq. (1) (nonprestressed)

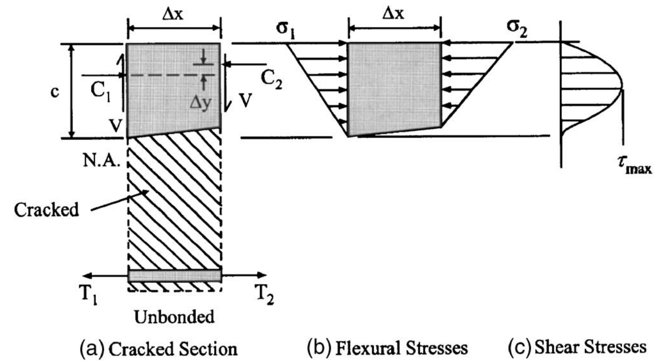

Fig. 3. Free body diagram at cracked section

inforced concrete members to prestressed concrete members. A primary goal was to develop a simple design procedure that can be used for the calculation of shear strength for both nonprestressed and prestressed sections enabling unification and simplification of design procedures.

Shear Strength

For prestressed members, there are two primary modes of cracking in shear: web shear and flexure shear. Web-shear cracking initiates in locations of high shear that are also subjected to low flexural stress. This cracking mode is typically observed in the end regions of thin-webbed prestressed members and occurs when the principal tensile stresses in the web exceed the tensile strength of the concrete. According to the ACI code (ACI 318 2005), the web-shear strength (V_{cw}) can be computed according to Eq. (3*a*). Alternately, a principal stress analysis can be conducted considering an assumed concrete tensile strength limit of $4\sqrt{f'_c}$ $(0.33\sqrt{f'_c})$

$$V_{cw} = (3.5\sqrt{f'_c} + 0.3f_{pc})b_w d_p + V_p \tag{3a}$$

$$(V_{cw} = (0.29\sqrt{f'_c} + 0.3f_{pc})b_w d_p + V_p) \tag{3b}$$

Flexure-shear cracking is the result of shear causing flexural cracks to "turn over" and incline towards the loading due to inclined tension cracking. According to the ACI code, the flexure-shear strength (V_{ci}) can be computed according to Eq. (4*a*)

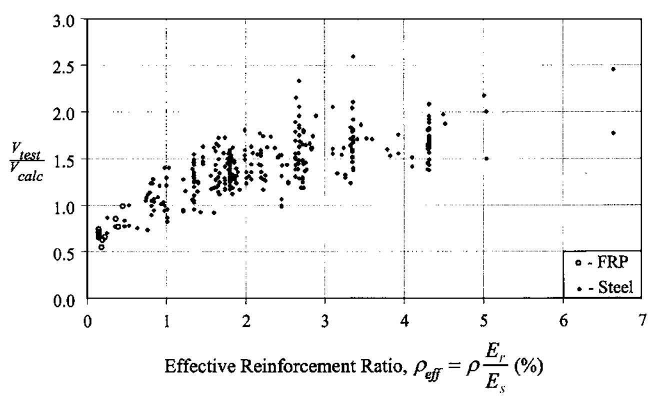

Fig. 2. Results of Eq. (2) (nonprestressed)

$$V_{ci} = 0.6\sqrt{f'_c}b_w d_p + V_d + \frac{V_i M_{cre}}{M_{max}} \geqslant 1.7\sqrt{f'_c}b_w d_p \tag{4a}$$

$$\left(V_{ci} = 0.05\sqrt{f'_c}b_w d_p + V_d + \frac{V_i M_{cre}}{M_{max}} \geqslant 0.14\sqrt{f'_c}b_w d_p\right) \tag{4b}$$

While both modes must be considered, the focus of this research study is on the flexural-shear strength.

Prestressed Beam Database

A database of prestressed concrete sections was generated to evaluate the applicability of the shear model. Composed of rectangular and I-sections without transverse reinforcement from tests conducted by Sozen, Zwoyer, and Siess (Sozen et al. 1959), the database was examined to eliminate failures which were not caused by diagonal tension. A total of nine sections were eliminated because they were reported to have failed in flexure while four sections were eliminated because they showed signs of web shear. In these four sections, diagonal-tension cracks formed in locations where flexural cracks were not present. Considering only diagonal-tension failures, the database contained 37 rectangular sections and 49 I-sections. The range of variables for these specimens is as follows: concrete strength, f_c, from 1,750 to 7,990 psi (12.1–55.1 MPa), effective depth, d, from 8.0 to 11.1 in. (203–282 mm), and a/d ratio from 2.70 to 6.73. All specimens were simply supported and tested with either one or two concentrated loads to provide regions of constant shear. It is interesting to note that these are the same specimens that were considered in the development of the existing ACI provisions.

Shear Model Analysis

In the current ACI 318 design equation, the effective area which resists shear is $b_w d$. The proposed shear model, however, provides a different effective shear area for the calculation of V_{ci}. A free body diagram at a cracked section is shown in Fig. 3. Because the cracked concrete cannot provide bond to the tension reinforcement, the tension force (T) must remain constant over the crack width Δx. To maintain horizontal equilibrium, the compression force (C) must also be constant over the cracked section. Considering moment equilibrium, a shear couple ($V\Delta x$) is present on the section. To resist this moment, the resultant of the compressive force on the larger moment side shifts upward. This is accomplished by shifting the neutral axis upward and increasing the

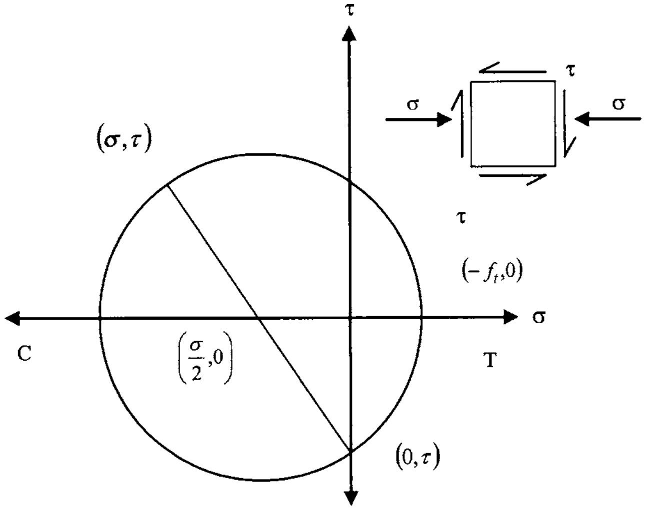

Fig. 4. Mohr's circle

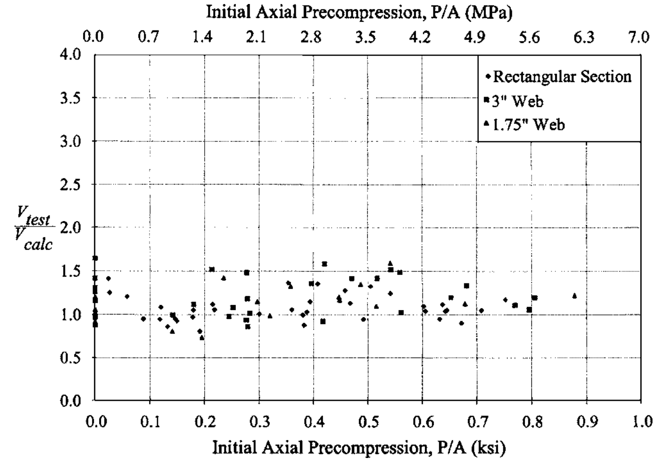

Fig. 5. Comparison of shear model with test results

flexural stress, creating the moment $C\Delta y$. Consequently, a shear stress distribution, shown in Fig. 3, is created from this shift and is distributed through the compression zone. The shear stresses were computed considering equilibrium of horizontal slices across Δx. According to this model, shear resistance is provided through the compression zone at the cracked section.

Considering the flexural and shear stress distributions (Fig. 3), each point along the depth of the section has a corresponding flexural stress (σ) and shear stress (τ). For this state of stress, the principal tensile stress was determined from Mohr's circle (Fig. 4) according to Eq. (5)

$$-f_t = \frac{\sigma}{2} - \sqrt{\left(\frac{\sigma}{2}\right)^2 + \tau^2} \tag{5}$$

Eq. (5) can be solved for the shear stress resulting in Eq. (6). The critical shear stress (τ_{cr}) that causes cracking in the compression zone is determined by setting the principal tensile stress equal to the tensile strength (f_{ct}) of the concrete

$$\tau_{cr} = \sqrt{\left(\frac{\sigma}{2} + f_{ct}\right)^2 - \left(\frac{\sigma}{2}\right)^2} \tag{6}$$

The flexural stress, σ, at each location along the depth of the compression zone was substituted into Eq. (6) to evaluate the corresponding τ_{cr}. If the applied τ as provided from the shear stress distribution exceeds τ_{cr}, a crack can form inside the compression zone. This process was repeated for increasing levels of moment above the cracking moment until a crack developed in the compression zone. Crack initiation inside the compression zone was identified as causing a flexure-shear failure.

The accuracy of the shear model analysis is dependent on the assumptions on which it was based. The primary assumptions for this analysis were the stress-strain relationship and the tensile strength of concrete. The stress-strain relationship for concrete was taken as Eq. (7) as provided by Hognestad (Lin and Burns 1981). The tensile strength of concrete was taken as $6\sqrt{f_c'}$ $(0.5\sqrt{f_c'})$ which is consistent with the derivation of the shear model provided for reinforced sections (Tureyen and Frosch 2003)

$$\sigma = f_c'\left[\frac{2\varepsilon}{\varepsilon_0} - \left(\frac{\varepsilon}{\varepsilon_0}\right)^2\right] \tag{7}$$

Using this analysis method, the shear strength of the specimens included in the database was calculated (Wolf 2003). As shown in Fig. 5, the measured shear strength was divided by the calculated shear strength for each specimen and plotted versus the initial axial precompression. The initial axial precompression shown is the compressive stress in the concrete (after allowance for all prestress losses) at the centroid of the section.

While this method is fairly accurate, it can be noted that the shear strength of several sections is unconservative. The primary cause of this overestimation of shear strength is the assumed tensile strength, $6\sqrt{f_c'}$ $(0.5\sqrt{f_c'})$. If a lower value of tensile strength is used, it is possible to increase the level of conservatism to any level desired.

For comparison purposes, the shear strengths of the specimens were also calculated using the ACI approach [Eq. (4)]. As shown in Fig. 6, slightly more scatter is provided by this approach. In particular, there is an inconsistency in the accuracy provided for nonprestresssed sections as compared with the prestressed. A statistical comparison of the results is provided in Table 1. These results indicate that the proposed shear model provides reasonable results while providing a means to unify the calculation procedure for nonprestressed and prestressed sections.

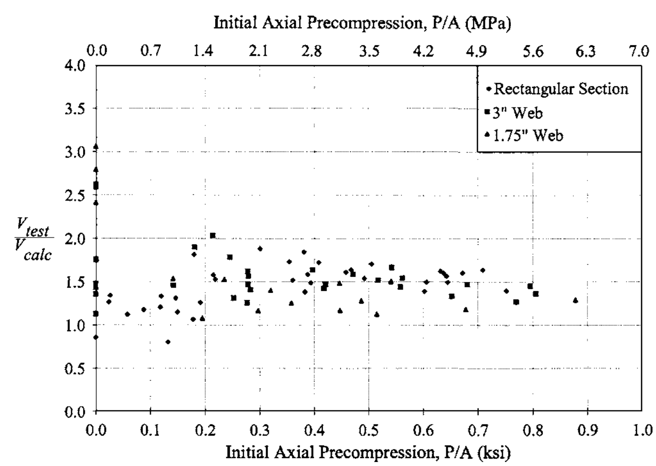

Fig. 6. Comparison of ACI method with test results

Table 1. Statistical Results

Section shape	Statistical parameter	Calculation method		
		ACI 318	Shear model	Design equation
Rectangular	Average	1.45	1.08	1.49
	SD	0.26	0.15	0.22
	COV	0.18	0.14	0.15
I-Section	Average	1.62	1.18	1.45
	SD	0.48	0.22	0.23
	COV	0.30	0.19	0.16
All	Average	1.55	1.14	1.47
	SD	0.40	0.20	0.23
	COV	0.26	0.18	0.16

Simplified Method

While the results provided by the shear model analysis compare very well with the test results, multiple calculations are required to determine V_{ci} which can be time consuming. Therefore, an investigation was performed to simplify the shear model for design purposes. Rather than analyzing local stresses over the depth of the compression zone, the goal of this investigation was to determine an average shear strength that causes a flexure-shear failure.

To determine the average shear strength, the rectangular specimens from the prestressed beam database were isolated to determine a coefficient of $\sqrt{f_c'}$, defined as K, which would provide conservative results. Considering an average shear strength over the compression zone, the equation for shear strength can be represented as

$$V_{ci} = K\sqrt{f_c'}b_w c \tag{8}$$

For the initial investigation, only rectangular sections were considered. For rectangular sections, an average shear stress can be considered over the entire compression zone. I-beams in the database were not considered because the contribution of the flanges to shear strength was uncertain. Considering the analytical results for V_{ci}, K was computed for each specimen using the neutral axis depth, c, that corresponds to the applied moment at the predicted failure shear. The resulting K was plotted as shown in Fig. 7. As shown, the analytical K values range from approximately 5 to 10.

Considering Eq. (6), shear strength is a function of the flexural stress in the compression zone. Therefore, K was defined in terms of the applied moment to account for the influence of flexural stress on flexure-shear strength. The general equation for K was considered as

$$K = 5 + \alpha(\nu - 1) \tag{9}$$

where α=variable to modify for the influence of flexural stress on shear strength; and v=multiple of the cracking moment, $M_{applied}/M_{cr}$.

After investigating varying α values, α equal to 0 was selected because it returned consistent, conservative results. Therefore, Eq. (9) simplifies to K=5 and is independent of the applied moment. Consequently, flexure-shear strength can be estimated using Eq. (10). This equation is identical to that proposed for nonprestressed sections [Eq. (1)]

$$V_{ci} = 5\sqrt{f_c'}b_w c \quad (V_{ci} = 0.42\sqrt{f_c'}b_w c) \tag{10}$$

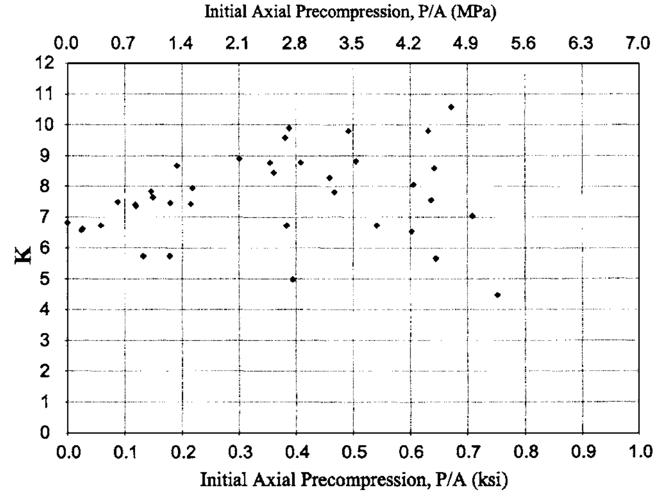

Fig. 7. K factors

While this simplification provides ease for the determination of the shear strength of rectangular sections, a complication still exists for flanged sections regarding the appropriate area of the compression zone that should be considered. A database of 150 nonprestressed concrete sections (Kani 1979; Placas and Regan 1971; Farmer and Ferguson 1967; Laupa et al. 1953) was used to determine the contribution of the flanges to flexure-shear strength. Nonprestressed concrete T-beams were evaluated because, unlike prestressed concrete sections, the neutral axis depth of reinforced concrete sections is constant for moments above the cracking moment which allows it to be eliminated as a variable in the analysis to determine an effective shear area. Shear failures in reinforced beams are considered prior to flexural yielding as well as being located in lower flexural stress regions; therefore, neutral axis migration following yielding does not have to be considered. For prestressed sections on the other hand, the initial tension generated by prestressing causes the neutral axis depth to vary with increasing applied moments. At the cracking moment, the neutral axis depth of a section is deeper in the section than the neutral axis depth at a higher moment.

Knowing the shear which caused the beam to fail, the required effective shear resistance area can be determined (Tureyen et al. 2006). The effective shear resistance area (A_{eff}) is composed of the web portion of the compression zone and an additional area of the flange. Several investigations were performed to determine a conservative, simple method to evaluate A_{eff}. It was determined that the contribution of the flanges should be limited by an effective flange width ($b_{eff,v}$), similar to current provisions used for flexure in ACI 318. Using the T-beam database, the effective flange width for shear was defined as

$$b_{eff,v} = b_w + t_f \tag{11}$$

An example of the effective shear area is shown in Fig. 8. For rectangular sections A_{eff} is equal to $b_w c$. For flanged sections, if the neutral axis is located in the web, A_{eff} is equal to $b_w c$ plus, t_f^2. If the neutral axis is located in the upper flange, A_{eff} is equal to $b_{eff,v}c$.

Considering an average shear strength ($K\sqrt{f_c'}$), the number of calculations required to evaluate the shear strength of a prestressed section is significantly reduced. Using the simplified analysis, the neutral axis depth at a given moment is the only calculation required. Once the neutral axis depth is known, A_{eff}

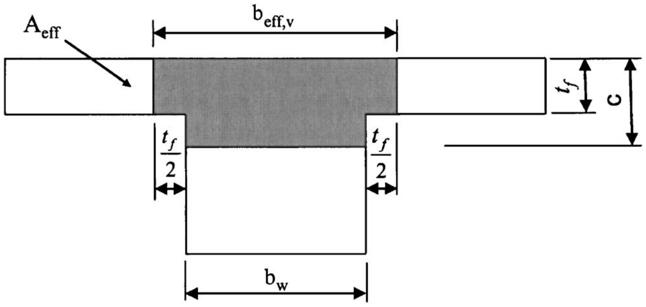

Fig. 8. Effective shear area

can be easily determined, and the shear strength can be computed as the average shear strength, $5\sqrt{f_c'}$ $(0.42\sqrt{f_c'})$ times the effective shear area A_{eff} [Eq. (12)]

$$V_{\text{ci}} = 5\sqrt{f_c'}A_{\text{eff}} \quad (V_{\text{ci}} = 0.42\sqrt{f_c'}A_{\text{eff}}) \tag{12}$$

This simplified method was used to compute the shear strengths of the beams included in the prestressed beam database to evaluate its performance. The measured shear strengths were again divided by the computed shear strengths and plotted versus the initial axial precompression (Fig. 9). As shown, the simplified method provides consistent and conservative results across the range of axial precompression included in the database. Furthermore, it performs with nearly the same level of accuracy as the complete shear model (Fig. 5). The statistical results in Table 1 also support the excellent performance of this expression. It should be noted that the equation performs equally well for both rectangular and flanged sections.

As reflected by the range of variables considered in the database, consistent results are provided across a range of concrete strengths, initial axial precompression stresses, and a/d ratios. Unfortunately, it was not possible to evaluate the presence of a size effect as the effective depths only ranged from 8.0 to 11.1 in. (203–282 mm). However, analysis of the reinforced concrete database (Tureyen and Frosch 2003) demonstrates that the use of an average shear strength of $5\sqrt{f_c'}$ $(0.42\sqrt{f_c'})$ provides a lower bound across a range of effective depths from 4.3 to 43.2 in. (102–1,097 mm). Additional testing is needed for larger prestressed beams unreinforced in shear.

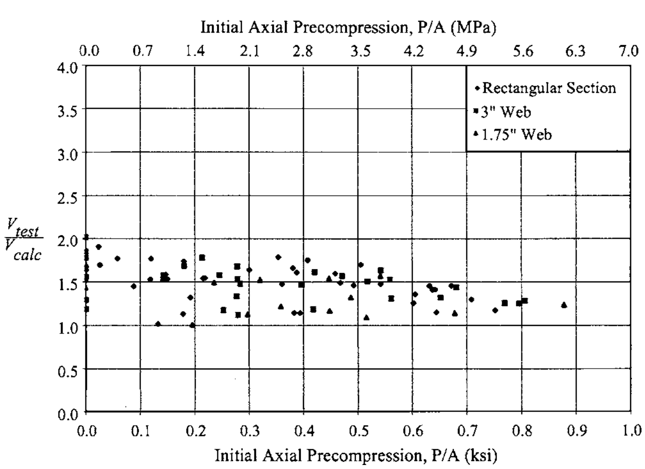

Fig. 9. Comparison of design equation [Eq. (12)] with test results

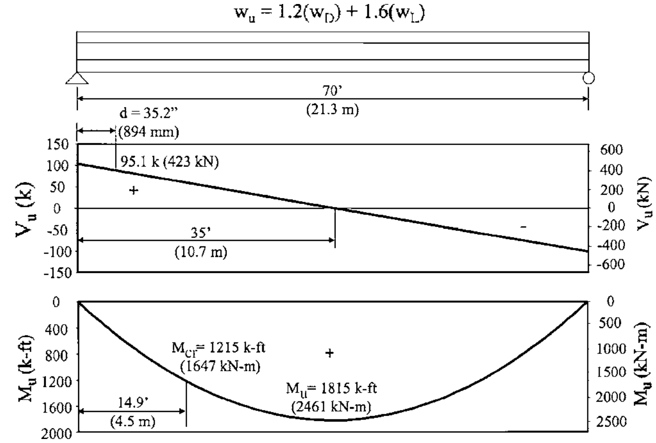

Fig. 10. Design example

Design Example

To illustrate the design process using the proposed design expression as well as to compare with results provided by current practice, an example problem was evaluated. Consider a simply supported beam subjected to a dead load of 0.45 kip/ft (6.6 N/mm) and a live load of 1.5 kip/ft (22 N/mm) over its entire 70 ft (21.3 m) span (Fig. 10). The moments and shears for this loading were computed based on the ACI 318-05 load and resistance factors. Based on the moment diagram, the cross section was appropriately sized. Material properties and dimensions, as well as the effective flange width for shear, are shown in Fig. 11. Because the effective flange width is only a function of section geometry, it can be determined directly for the cross-sectional dimensions. Consequently, the effective shear area is simply a function of the neutral axis depth.

As stated earlier, the neutral axis depth of prestressed concrete sections varies with applied moment. Therefore, the neutral axis depth and subsequently the shear strength are dependent on the applied moment. For each section along the length of the beam, the neutral axis depth was calculated based on the factored mo-

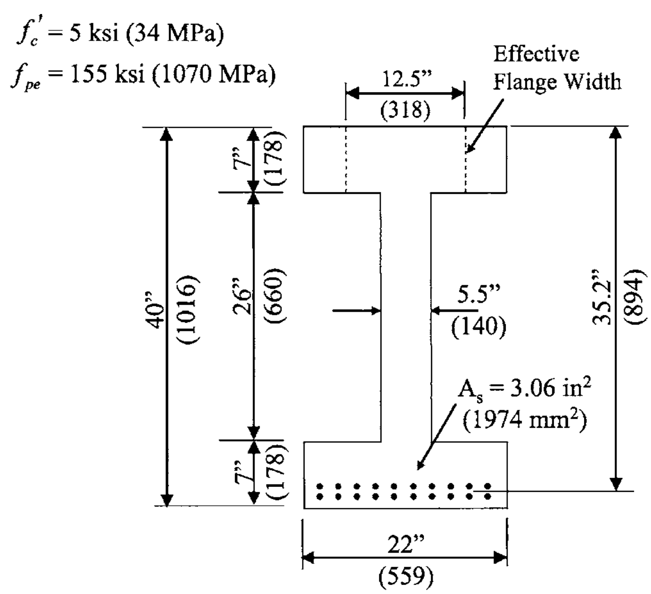

Fig. 11. Selected cross section

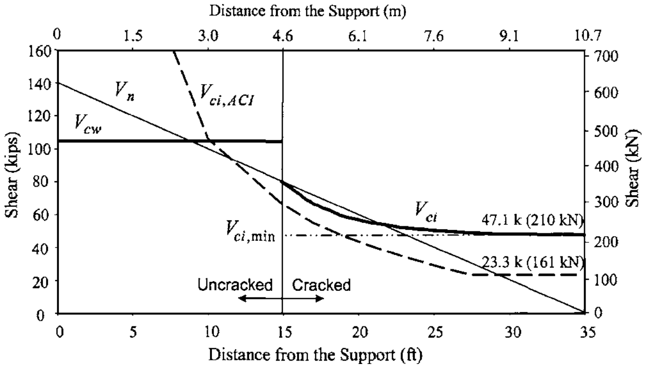

Fig. 12. Design shear strengths

ment at that location using a strain-compatibility analysis. For sections where the moment is greater than or equal to the cracking moment, the shear strength is controlled by flexure-shear (V_{ci}). For these regions, the shear strength was computed according to Eq. (12). The effective shear area, A_{eff}, was determined over the length of the beam based on the computed neutral axis depth at that location. For moments less than the cracking moment, the section is not cracked and the shear strength is controlled by web shear (V_{cw}) which was computed according to the alternative method provided by ACI. The shear strengths computed using the proposed method are plotted in Fig. 12. As shown, the shear strength drops as the moment is increased with the lowest capacity being calculated at midspan. For comparison, the flexure-shear strength calculated using ACI 318 ($V_{ci,ACI}$) is also provided. For locations greater than approximately 27 ft (8.2 m) from the support, the ACI minimum, $1.7\sqrt{f_c'}b_wc$ $(0.14\sqrt{f_c'}b_wc)$, controls. Overall, the shear strength calculated using the proposed method follows the same trend as the ACI method but computes shear strengths consistently higher than that computed using the ACI 318 method. While this provides less conservatism than current practice, the proposed method is conservative as previously discussed.

As an alternative procedure, rather than computing V_{ci}, over the length of the beam, only the minimum shear strength needs to be calculated. This alternative procedure provides a uniform and conservative shear strength for locations where the applied moment exceeds the cracking moment. Furthermore, it provides simplification in that only one neutral axis depth need be considered.

For this example, the concrete alone is not capable of resisting the applied shear. At locations where the applied shear exceeds the shear strength ($V_n > V_c$), transverse reinforcement should be provided to prevent a shear failure. The spacing and amount of the vertical reinforcement should be determined such that $V_n = V_c + V_s$ as currently provided by the ACI 318 provisions. The concrete contribution V_{ci} or V_{cw}, as appropriate, is added to the shear reinforcement contribution V_s to provide the total shear strength.

Calculation of V_{cw}

As previously discussed, ACI 318 provides two methods for the calculation of web-shear strength in prestressed members. The alternative approach provided in ACI 318, Section 11.4.3.2 provides for a principal stress analysis of an uncracked section. Using a tensile strength of $4\sqrt{f_c'}$ $(0.33\sqrt{f_c'})$, the web-shear strength of the section can be determined. The other approach is provided by Eq. (3) [ACI 318, Eq. (11–12)]. This equation provides an approximation of the principal stress analysis (Lin and Burns 1981). For the design example, the web-shear strength, $V_{cw} = 105$ kips (467 kN), is presented based on that calculated using the alternative approach recommended by ACI 318. Similar results are provided if Eq. (3) is used [$V_{cw} = 109$ kips (485 kN)].

It should be noted that the ACI approach used to calculate web-shear strength is based on mechanics using a principal stress analysis. This analysis of the uncracked section is consistent with the shear strength model presented by Tureyen and Frosch (2003) and the shear model presented here for analysis of flexure-shear strength. However, for consideration of flexure-shear strength, a principal stress analysis is conducted for the cracked section. While ACI 318 recommends a tensile strength of $4\sqrt{f_c'}$ $(0.33\sqrt{f_c'})$ for the web shear analysis, the shear model was developed using a tensile strength of $6\sqrt{f_c'}$ $(0.5\sqrt{f_c'})$. A tensile strength of $6\sqrt{f_c'}$ $(0.5\sqrt{f_c'})$ is reasonable for analysis purposes; however, a lower value such as suggested by ACI is appropriate to provide conservatism as discussed earlier and illustrated by Fig. 5.

Comparison of Design Methods

The primary difference between the proposed design equation and the ACI 318 approach is at the transition where the flexure-shear strength begins to control. When calculating shear strength using ACI 318, both V_{ci} and V_{cw} are calculated over the length of the beam with the lesser of the two controlling. Therefore, the flexure-shear strength can control design even in portions of the beam which have a factored applied moment less than the cracking moment. The proposed design equation calculates shear strength differently. This equation considers that flexure-shear cracks initiate as flexural cracks. With sufficient shear, these flexural cracks turn into flexure-shear cracks and ultimately produce a flexure-shear failure (Lin and Burns 1981; ACI 318 2005). Therefore, flexure-shear failure cannot occur where flexural cracks are not present such as where the applied moment is less than the cracking moment. For locations where the applied moment is less than the cracking moment, the shear strength is controlled by web shear. At moments greater than the cracking moment, the lower of the flexure-shear and web-shear strength controls.

Summary and Conclusions

A shear model was used to analyze a database of 86 prestressed specimens which were tested in shear. The combination of flexural and shear stresses in the compression zone of the cracked section were calculated and principal tension stresses were determined to evaluate the shear strength of the section. Through this analysis, it was concluded that the shear model is applicable to prestressed concrete sections and provides a fairly accurate method to calculate the flexure-shear strength (V_{ci}) of prestressed concrete. Consistent results were obtained over the range of initial axial precompression stresses available in the database.

Although the shear model is applicable to prestressed concrete, the analysis procedure is not practical for design purposes. An investigation was conducted to simplify the model considering both rectangular and flanged cross sections. It was determined that simplification could be achieved in the calculation of flexure-shear strength by considering an average shear strength of $5\sqrt{f_c'}$ $(0.42\sqrt{f_c'})$ over the compression zone. This method can be extended for flanged sections through the use of an effective shear resistance area (A_{eff}). As illustrated in Fig. 8, the effective shear area consists of the web portion of the compression zone plus an additional effective flange width. The effective flange width should not exceed $0.5t_f$ on either side of the web.

Analysis of the prestressed beam database indicates that the simplified design equation provides an accurate and conservative method for the calculation of the shear strength of prestressed sections considering a wide range of effective prestress levels. The design equation [Eq. (12)] is identical to that previously proposed for nonprestressed sections (Tureyen and Frosch 2003) indicating that unification can be provided for the calculation of shear strength in both reinforced and prestressed members. Furthermore, as illustrated by the design example, the calculation of shear strength provides consistency with expected behavior. Flexure-shear strength is only calculated at sections where the factored applied moment exceeds the cracking moment. Below the cracking moment, the section is controlled by web-shear strength.

Design Recommendations

Based on these findings, the following equation can be used to compute the flexure-shear strength for both nonprestressed and prestressed sections

$$V_{ci} = 5\sqrt{f'_c}A_{eff} \quad (V_{ci} = 0.42\sqrt{f'_c}A_{eff}) \tag{13}$$

Where the applied moment is greater than the cracking moment, the flexure-shear strength (V_{ci}) should be computed at multiple points along the length of the beam based upon the neutral axis depth determined from a strain-compatibility analysis. If design simplification is desired, only the minimum shear strength is required to be considered and can be computed based upon the neutral axis depth at the largest applied moment. Where the applied moment is less than the cracking moment, the current ACI 318 provisions should be used to calculate the web-shear strength (V_{cw}) of the section.

Acknowledgments

This investigation was conducted at Purdue University, West Lafayette, Ind. and was made possible under the sponsorship of the Indiana Department of Transportation (INDOT) and the Federal Highway Administration (FHWA) through the Joint Transportation Research Program (JTRP), Project No. SPR-2798. Their support is gratefully acknowledged.

Notation

The following symbols are used in this paper:

A_{eff} = effective shear area [in.^{2} (mm^2)];
b_w = beam width [in. (mm)];
c = cracked transformed section neutral axis depth [in. (mm)];
d = effective depth [in. (mm)];
d_p = distance from extreme compression fiber to centroid of prestressing steel [in. (mm)];
E_r = modulus of elasticity of reinforcement [psi (MPa)];
E_s = modulus of elasticity of steel [psi (MPa)];
f'_c = specified compressive strength of concrete [psi (MPa)];
f_d = stress due to unfactored dead load, at extreme fiber of section where tensile stress is caused by externally applied loads [psi (MPa)];
f_{pc} = compressive stress in concrete (after allowance for all prestress losses) at centroid of cross section resisting externally applied loads or at junction of web and flange when centroid lies within flange [psi (MPa)];
f_{pe} = compressive stress in concrete due to effective prestress forces only (after allowance for all prestress losses) at extreme fiber of section where tensile stress is caused by externally applied loads [psi (MPa)];
I = moment of inertia of section about centroidal axis [in.^{4} (mm^4)];
M_{cre} = moment causing flexural cracking at section due to externally applied loads [in.·lb (N mm)] $I/y_t(6\sqrt{f'_c}+f_{pe}-f_d)(I/y_t(0.5\sqrt{f'_c}+f_{pe}-f_d))$;
M_{max} = maximum factored moment at section due to externally applied loads [in.·lb (N mm)];
V_c = nominal shear strength provided by concrete [lb (N)];
V_d = shear force at section due to unfactored dead load [lb (N)];
V_i = factored shear force at section due to externally applied loads occurring simultaneously with M_{max} [lb (N)];
V_n = nominal shear strength [lb (N)];
V_p = vertical component of effective prestress force at section [lb (N)];
V_s = nominal shear strength provided by shear reinforcement [lb (N)]; and
y_t = distance from centroidal axis of gross section, neglecting reinforcement, to tension face [in. (mm)].

References

AASHTO. (2002). *Standard specifications for highway bridges*, 17th Ed., Washington, D.C.

AASHTO. (2005). *AASHTO LRFD bridge design specifications*, Washington, D.C.

American Concrete Institute (ACI) Committee 318. (2005). "Building code requirements for structural concrete (ACI 318-05) and Commentary." *ACI 318R-0*, Farmington Hills, Mich.

Farmer, L. E., and Ferguson, P. M. (1967). "T-beams under combined bending, shear, and torsion." *ACI J.*, 64(11), 757–766.

Kani, M. W. (1979). *Kani on shear in reinforced concrete*, Dept. of Civil Engineering, University of Toronto Press, Toronto.

Laupa, A., Siess, C. P., and Newmark, N. M. (1953). "Strength in shear of reinforced concrete beams." *Engineering Experiment Station Bulletin No. 428*, Univ. of Illinois, Champaign, Ill.

Lin, T. Y., and Burns, N. H. (1981). *Design of prestressed concrete structures*, 3rd Ed., Wiley, New York.

National Cooperative Highway Research Program (NCHRP). (2002). "Simplified shear design of structural concrete members." *Project 12-61*, Washington, D.C.. ⟨http://www4.nationalacademies.org/trb/crp.nsf/All+Projects/NCHRP+12-61⟩.

Placas, A., and Regan, E. P. (1971). "Shear failure of reinforced concrete beams." *ACI J.*, 68(10), 763–773.

Reineck, K. H., Kuchma, D. A., Kim, K. A., and Marx, S. (2003). "Shear database for reinforced concrete members without shear reinforce-

ment." *ACI Struct. J.*, 100(2), 240–249.
Sozen, M. A., Zwoyer, E. M., and Siess, C. P. (1959). "Strength in shear of beams without web reinforcement." *Engineering Experiment Station Bulletin*, *No. 452*, Univ. of Illinois, Champaign, Ill.
Tompos, E. J., and Frosch, R. J. (2002). "Influence of beam size, longitudinal reinforcement, and stirrup effectiveness on concrete shear strength." *ACI Struct. J.*, 99(5), 559–567.
Tureyen, A. K., and Frosch, R. J. (2003). "Concrete shear strength: Another perspective." *ACI Struct. J.*, 100(5), 609–615.
Tureyen, A. K., Wolf, T. S., and Frosch, R. J. (2006). "Shear strength of reinforced concrete T-beams without transverse reinforcement." *ACI Struct. J.*, 103(5), 656–663.
Wolf, T. S. (2003). "Simplified design for shear of prestressed concrete members." Master's thesis, Purdue Univ., West Lafayette, Ind.